PHYSOR 2002, Seoul, Korea, October 7-10, 2002

POSITIVE LINEAR AND NONLINEAR SURFACE CHARACTERISTIC SCHEMES FOR THE NEUTRON TRANSPORT EQUATION IN UNSTRUCTURED GEOMETRIES

S. Santandrea and R. Sanchez

Direction de l'Energie Nucléaire
Service des Etudes de Réacteurs et de Modélisation Avancée
CEA de Saclay
France
simone.santandrea@cea.fr , richard.sanchez@cea.fr

ABSTRACT

In this paper we present two new numerical schemes for the method of characteristic in unstructured geometries (MOC) for the neutron transport equation. The MOC has become a familiar tool for transport calculations in reactor physics [1], and its use will probably increase in the future. One of the major drawbacks of the MOC is the difficulty to implement higher-order integration schemes to improve spatial convergence. We present here two high-order schemes for the MOC, the second being a direct generalization of the first. We define a positive, linear characteristic scheme based on linear interpolation on the surface's values of the collisions sources. We have called it Linear Surface (LS) scheme. Results comparisons of the well-known Stepanek benchmark show LS faster convergence over the standard step characteristic scheme. A generalization of the synthetic ASA acceleration scheme provides an efficient method to accelerate the internal transport iterations. However, the LS scheme is not conservative. To improve this scheme we have adopted a nonlinear rebalancing procedure. The result is a Non-Linear Surface (NLS) scheme permitting linear variation of the source but also source discontinuities that enforce neutron conservation. The comparisons of the results for the Stepanek benchmark show that this method is much better with respect to spatial convergence. Unfortunately the nonlinear nature of the scheme complicates the conception of an acceleration method.

1. INTRODUCTION

The method of characteristic in unstructured meshes (MOC) has become a familiar tool for transport calculations in reactor physics [1]. This method uses numerical trajectories to construct an iterative solution of the transport equation based on the exact cell-balance and propagation equations. The drawback of the method is the difficulty of implementing positive high-order source approximations in arbitrarily shaped regions. The use of polynomial flux expansions does not yield a positive scheme and, therefore, robust methods are based on the flat-flux approximation. Exponential interpolation can be used to restore positivity [3], to the prize of introducing a non-linearity that requires extra tabulations (in regular meshes) or Newton iterations (in unstructured meshes). Moreover, the exponential

approximation does not respect the basic linearity of the transport equation (i.e., a linear combination of solutions must be a solution) and, therefore, poses problems in its utilization in multigroup calculations.

In this paper we present a new MOC linear surface (LS) scheme that is linear, positive and respects linearity. The central idea is to replace the flat source region approximation with a linear interpolation between surfaces values. We have also generalized the ASA acceleration technique, developed for the flat source scheme, to accelerate the LS internal iterations. A Fourier analysis for heterogeneous slabs, not presented in this paper, proved that this new acceleration is stable and efficient. However, the LS scheme is not conservative, although it converges to the exact solution as the mesh size is refined. This means that the default in balance goes to zero with the mesh size. A second, positive, conservative nonlinear surface scheme (NLS) can be obtained by renormalizing the LS equations. This new scheme proves to be very efficient but a stable acceleration has still to be found.

2. THE STEP CHARACTERISTICS SCHEME (SC)

The MOC for unstructured meshes applies the discrete ordinate approximation to obtain a numerical iterative solution of the one group transport equation in a geometrical domain D of boundary ∂D:

$$\left.\begin{aligned} (\Omega\cdot\nabla+\Sigma)y^{(n)} &= q^{(n-1)}, \quad x\in X, \\ y^{(n)} &= by^{(n-1)}+y_0, \qquad x\in \partial_- X, \end{aligned}\right\} \tag{1}$$

where n denotes the iteration index, x=(r,Ω) stands for a generic point in phase space $X=\{x; r\in D, \Omega\in(4p)\}$, Σ is the total cross section and

$$q = Hy + S \tag{2}$$

is the emission density, where $(Hy)(x)=\int_{(4p)} d\Omega'\Sigma_s(r,\Omega\cdot\Omega')y(r,\Omega')$ is the scattering operator and S the external source.

In the method of characteristics the discrete ordinates scheme is used for the angular approximation, so that each integration over the angular variable is calculated as:

$$S_N=\{w_n,\Omega_n,n=1,N\}\Rightarrow\frac{1}{4p}\int_{(4p)} f(\Omega)d\Omega\sim\sum_n w_n f(\Omega_n), \tag{3}$$

where w_n is the angular weight associated to direction Ω. In the classic Step Characteristics (SC) method the geometrical domain D is decomposed into a set of homogeneous regions $\{D_i, i=1, N_{reg}\}$ on which we use the flat source approximation. As it is shown for example in [2] we can give the following representation to the collision term:

$$q(x)\sim\sum_i q_i(r)q_i(\Omega)=\sum_i q_i(r)\vec{A}(\Omega)\vec{q}_i(\Omega), x\in X, \tag{4}$$

where q_i is the characteristics function of homogeneous region D_i and

$$\vec{q}_i = \Sigma_{si}\vec{f}_i + \vec{S}_i \tag{4a}$$

is the average value of the emission density in region i. In a multigroup setting, the external source accounts for fissions and scattering from the other groups.

A set of parallel numerical trajectories is constructed for each angular direction in the angular quadrature formula (3) and an iterative solution of the transport equation is then obtained from boundary flux values by direct integration along each numerical trajectory. Over one of these trajectories, the flux can be expressed as:

$$y_{out}(x,\Omega) = e^{-t(x_{in},x)} y_{in}(x_{in},\Omega) + \int_{x_{in}}^{x} e^{-t(x',x)} q(x',\Omega)dx', \tag{5}$$

where x indicates the position along the trajectory, x_{in} is the entering point of the trajectory in the domain and $t(x',x)$ is the optical distance along the trajectory between point x and x'. In the SC method, equation (5) can be directly integrated, thanks to the flat source approximation, to give:

$$y^{(n)}_{out,i}(i) = e^{-\Sigma_i R_i(t)} y^{(n)}_{in,i}(t) + \underbrace{\frac{1-e^{-\Sigma_i R_i(t)}}{\Sigma_i}}_{b(R_i)} q_i^{(n-1)}(\Omega), \tag{6}$$

where $R_i(t)$ is the length of the trajectory within the region i and Ω is the direction of trajectory t. This equation is used to compute iteratively the angular flux across the cells along each trajectory.

The updating of the flux moments is made via the angular flux:

$$\vec{f}_i^{(n)} = \sum_n w_n \vec{A}(\Omega_n) y_i^{(n)}(\Omega_n),$$

where $y_i^{(n)}(\Omega_n)$ are the cell mean angular fluxes that are defined by the cell balance equation:

$$\Sigma_i y_i^{(n)}(\Omega_n) = q_i^{(n-1)}(\Omega_n) - \frac{1}{V_i}\sum_{t\|\Omega, t\cap i} w_\perp(t)\left[y^{(n)}_{out,i}(t) - y^{(n)}_{in,i}(t)\right]. \tag{7}$$

Here V_i is the volume of the cell and the sum in t is done for all trajectories with direction Ω that intersect cell i. The $w_\wedge$ is the spatial integration weight, geometrically representing the area affected to the trajectory. We avoid, in this brief discussion, to discuss the treatment of boundary conditions that can be found in [2].

3. THE LS SCHEME

This scheme is based on a linear interpolation between cell boundary values of the collision source in the integral formula (5). To perform this integration one needs the value of the sources within each region. For a trajectory t crossing cell i in direction Ω we write:

$$q_t(x,\mathrm{W}) = q_t(0,\mathrm{W})\frac{x}{l} + q_t(l,\mathrm{W})(1-\frac{x}{l}), \tag{8}$$

where x is the distance along the trajectory and l the chord length in region i. Replacing (8) into (5) gives:

$$y^{(n)}_{out,i}(i) = e^{-\Sigma_i R_i(t)} y^{(n)}_{in,i}(t) + b(l) q^{(n-1)}_{t,i}(0,\Omega) + \underbrace{\frac{l - b(l)}{s\, l}}_{b_1(l)} \left(q^{(n-1)}_{t,i}(l,\Omega) - q^{(n-1)}_{t,i}(0,\Omega) \right), \quad (9)$$

where the symbol b has been implicitly defined in (6). One can also calculate the average flux over a chord length:

$$\begin{aligned} \bar{y}^{(n)}(t) &= \frac{1}{l}\int_0^l ds\, y\,(s) \\ &= b\,(l)\, y^{(n)}_{in,i}(t) + \frac{l - b\,(l)}{\Sigma} q^{(n-1)}_{t,i}(0,\Omega) + \frac{q^{(n-1)}_{t,i}(l,\Omega) - q^{(n-1)}_{t,i}(0,\Omega)}{\Sigma}[l/2 - b_1(l)]. \end{aligned} \quad (10)$$

The average chord flux in (10) can be used to express the average angular flux in region i by adding the contributions of all trajectories cutting this region with angle Ω:

$$\begin{aligned} \Sigma_i V_i \bar{y}^{(n)}_{i,C}(\Omega_n) &= \sum_{t \| \Omega, t \cap i} w_\perp(t) \Sigma_i \bar{y}^{(n)}_i(t) \\ &= \sum_{t \| \Omega, t \cap i} w_\perp(t) \left[\frac{q^{(n-1)}_{t,i}(l,\Omega) + q^{(n-1)}_{t,i}(0,\Omega)}{2} \cdot l + y^{(n)}_{in,i}(t) - y^{(n)}_{out,i}(t) \right] \\ &= \sum_{a \in i} \left(J^-_a - J^+_a \right)^{(n)}(\Omega) + V_i \bar{Q}^{(n-1)}_{i,G}(\Omega) \end{aligned} \quad (11)$$

The sum in a is done over all surfaces surrounding region i and we have used the following definitions of partial currents

$$J^\pm_a(\Omega) = \sum_{t \| \Omega, t \cap a} w_\perp(t) y^{(n)}_{\pm,i}(t) \sim \int_a dS \left| \Omega^\pm \cdot n \right| y\,(r, \Omega^\pm), \quad (12)$$

where the "+" and "-" stand for outgoing or ingoing angular directions. The definition of the geometrical source average has also been used:

$$\bar{Q}^{(n-1)}_{i,G}(\Omega) = \frac{1}{V_i} \sum_{t \| \Omega, t \cap i} w_\perp(t) \frac{q^{(n-1)}_{t,i}(l,\Omega) + q^{(n-1)}_{t,i}(0,\Omega)}{2} l = M(q_a). \quad (13)$$

Equation (13) implicitly defines the operator M of geometrical averaging. We have used subscripts "G" and "C" to denote that a quantity is obtained, respectively, from geometrical averaging or directly from the balance equation. Equation (11) looks like an angular balance equation and can be used to obtain volume average fluxes from surfaces sources. This equation is not a truly balance equation except at the limit when the mesh size goes to 0 and the geometrical mean $\bar{f}_{i,G}$ becomes equal to the balance value $\bar{f}_{i,C}$. This matter will be further discussed in the following.

Ultimately the value of the emission density q within a region depends on the inhomogeneous sources, if any, and on the multigroup fluxes via fission and scattering. For the LS scheme we have used a cell linear source approximation obtained by linear interpolation from cell surface values (a surface being the common boundary between two adjacent regions; but it can also be defined by further subdivisions to improve convergence). In practice we compute and store the average flux moments,

$$f_{kl}^{a} = \frac{1}{4p\,S_a}\int_{(a)} dS \int_{(4p)} d\Omega A_{kl}(\Omega) y\,(\mathbf{r},\Omega) \sim \frac{1}{S_a}\sum_{\substack{w_n \in S_N \\ t \cap S_a}} w_n \underbrace{\frac{w_\perp(t)}{|\Omega \cdot n|}}_{dS^t} A_k(\Omega_n) y_a^t(\Omega_n), \quad (14)$$

for each surface a and angular direction Ω. Here A_{kl} is the spherical harmonic of order (kl) and S_a is the area of a, and dS^t is the measure of the actual geometrical surface intersected by trajectory t. Formula (14) shows that all integrals are numerically evaluated using the angular fluxes along numerical trajectories. These fluxes are obtained by applying formula (9), during the transport sweep, and they are used to update the surface source that can be written as:

$$\vec{q}_a^{\pm} = \Sigma_{si,\pm}\vec{f}_a + \vec{S}_{a,\pm}, \quad (15)$$

where this source is computed for each cell because the cross sections are cell dependent.

In conclusion, the LS algorithm proceeds as follows:

1. Start with a guess surface source.
2. Make a transport sweep, calculate for each surface the moments of the flux with (14). Compute the current term in the pseudo-balance equation (11), and update volume fluxes.
3. Test convergence on volume and surface fluxes and eventually return to 1

We end this section with a discussion on the non-conservative nature of the LS algorithm. The "conservation' equation enforced in the LS scheme reads:

$$\Sigma_i V_i \overline{f}_{i,C}^{(n)} = \sum_{a \in i}\left(J_a^- - J_a^+\right)^{(n)} + V_i\left[\Sigma_{s,i}\overline{f}_{i,G}^{(n-1)} + Q_{ext\,i}\right], \quad (16)$$

whereas the true conservation equation requires the two average fluxes, $\overline{f}_{i,C}$ and $\overline{f}_{i,G}$, to be the same. Even at convergence of the iteration we are not granted that the "conservative" cell-average flux will equal the "geometrically" averaged one appearing in (16). What we have here is a solution where the sources are not coherent with the averaged values of fluxes. In a fully conservative scheme $\overline{f}_{i,C}^{(n)}, \overline{f}_{i,G}^{(n)}$ should converge to the same quantity, and this would satisfy the balance equation (16). However, even if the LS scheme is not conservative, it exhibits other interesting properties. First of all, since it uses a linear cell approximation for the sources, it is expected to be a high-order scheme. Secondly, the LS scheme is positive. This property is easy to see since the LS interpolation of the source is strictly positive obtained by linear interpolation of positive surface sources.. The later sources are positive because they computed from surface angular fluxes that are positive.

4. DP0 SYNTHETIC ACCELERATION OF THE LS SCHEME

The LS scheme is accelerated with a synthetic acceleration (ASA) based on uniform DP_0 surface angular fluxes [1]. To ensure numerical stability the LS scheme is carried over into the acceleration equations and all matrix coefficients are evaluated with the numerical trajectories. Since the idea of the ASA-type accelerations has been described elsewhere [2] for the standard SC scheme, we will give here only a brief description. The basic assumption is to suppose that the flux entering region i from a given surface b is isotropic:

$$y^{-}_{b}(\Omega) = \frac{J^{-}_{b}}{p S_{b}} = \hat{J}^{-}_{b}. \tag{17}$$

This assumption permits to express the average scalar flux on the surface b as:

$$f^{0}_{b} = \frac{\hat{J}^{-}_{b} + \hat{J}^{+}_{b}}{2}. \tag{18}$$

The ASA problem is posed for the normalized current defined in (17). This quantity is obtained from the integral transport equation:

$$\hat{J}^{+}_{a} = \frac{1}{p S_{a}} \int_{S_a} dS \int_{(2p+)} d\Omega |\Omega \cdot n| y\,(r,\Omega) = \sum_{b \in i} \left\{ T_{ab} \hat{J}^{+}_{b} + E^{1}_{ab} q_{b} \right\} + \overline{E}^{2}_{a} q_{a}, \tag{19}$$

where $\overline{E}^{2}_{a} = \sum_{b \in i} E^{2}_{ab}$ and where the following definitions for the transmission probabilities have been used:

$$\begin{aligned} T_{ab} &= \frac{1}{p S_{a}} \int_{S_a} dS \int_{(a \leftarrow b)} d\Omega |\Omega \cdot n| e^{-\Sigma_t l} \quad , \quad E^{1}_{ab} = \frac{1}{p S_{a}} \int_{S_a} dS \int_{(a \leftarrow b)} d\Omega |\Omega \cdot n| \left(b - \frac{l-b}{\Sigma_t l} \right), \\ E^{2}_{ab} &= \frac{1}{p S_{a}} \int_{S_a} dS \int_{(a \leftarrow b)} d\Omega |\Omega \cdot n| \frac{l-b}{\Sigma_t l}. \end{aligned} \tag{20}$$

All these quantities are calculated with the same numerical tracking used for the transport sweep in order to assure complete coherence and to grant stability. The quantity $\overline{E}^{2}_{a}$ is not computed from (20), but in order to enforce conservation is defined as:

$$\overline{E}^{2}_{a} = \frac{1 - \overline{T}_{a}}{\Sigma_{t}} - \overline{E}^{1}_{a}, \tag{21}$$

where $\overline{T}_{a} = \sum_{b} T_{ab}$ and $\overline{E}^{1}_{a} = \sum_{b} E^{1}_{ab}$. Finally, taking into account that in synthetic acceleration the source has the form:

$$\vec{q}^{\pm}_{a} = \Sigma_{si,\pm} \left(d\vec{f}_{a} + \Delta \vec{f}_{a} \right),$$

where $d\vec{f}_{a}$ is the correction to be searched, and $\Delta \vec{f}_{a} = f^{(n+1/2)} - f^{(n)}$ the difference between transport iterates, one gets:

$$\hat{J}^{+}_{a} = \sum_{b \in i} \left\{ \left[T_{ab} + \left(E^{1}_{ab} + d_{ab} \overline{E}^{2}_{a} \right) \frac{\Sigma_{s,i}}{2} \right] \hat{J}^{-}_{b} + \left[\left(E^{1}_{ab} + d_{ab} \overline{E}^{2}_{a} \right) \frac{\Sigma_{s,i}}{2} \right] \hat{J}^{+}_{b} + E^{1}_{ab} \frac{\Sigma_{s,i}}{2} \Delta f_{b} \right\} + \overline{E}^{2}_{a} \frac{\Sigma_{s,i}}{2} \Delta f_{a}, \tag{22}$$

where d_{ab} stands for the Kronecker's delta function.

System of equations (22) is solved iteratively with the help of the Biconjugate Gradient Stabilized Method [5]. Once convergence has been achieved, cells mean fluxes are obtained by adding the corrections to the last calculated transport surface fluxes:

$$f^{(n+1)} = df + f^{(n+1/2)} .$$

The DP0 acceleration is able to accelerate directly only the first moment, even if other moments can be taken into account by a scaling technique [1]. As for the treatment of boundary conditions, this is not differently implemented of the standard SC ASA acceleration and can be found in [1].

5. NON LINEAR SURFACE CHARACTERISTIC SCHEME

In order to enforce conservation, we have tried to impose this property in the LS scheme by a rescaling procedure. This procedure is based on the observation that conservation requires to modify the surface sources in such a way that their geometrical average coincide with the conservative average. At convergence the two averages will coincide, thus enforcing balance. The easiest way we have found to implement this idea has been to define the following rebalancing coefficients

$$f_i^{(n+1)} = \frac{M\left(f_a^{(n)}\right)}{\overline{f}_{i,C}^{(n)}}, \tag{23}$$

and to use these coefficients to renormalize the collision source for the iteration "*n+1*":

$$\vec{q}_{a,i}^{-,(n)} = f_i^{(n)} \Sigma_{si,-} \vec{f}_a^{(n)} + \vec{S}_{a,-}, \tag{24}$$

where α is one of the surfaces of region *i* and the source corresponds to the entering direction. When spatial convergence is fully attained the *f* rebalancing factors are expected to approach unity: actually the geometrical average fluxes for the LS scheme must converge to the spatially converged solution that is conservative. Formula (24) ensures that the geometrical average equals the conservative one:

$$M\left(q_a^{(n)}\right) = \overline{q}_{i,C}^{(n)} . \tag{25}$$

Since rebalancing is a non-linear process, we do not expect ASA synthetic acceleration for the LS scheme to be efficient. However, since when spatial convergence is sufficiently attained the *"f"* rebalancing coefficients are expected to approach unity, the ASA LS scheme could work well in such cases. Nevertheless, a stable efficient method to accelerate the NLS scheme is a subject for further research.

5. RESULTS FOR THE STEPANEK BENCHMARK

To test the performance of the new LS and NLS schemes we have considered the one-group source version of the Stepanek benchmark [3]. The geometry of this benchmark is that of a small reactor core comprising four central regions and an external moderator with vacuum boundary conditions. Figure 1 represents schematically the system. Isotropic and uniform sources are located in regions 1 and 3.

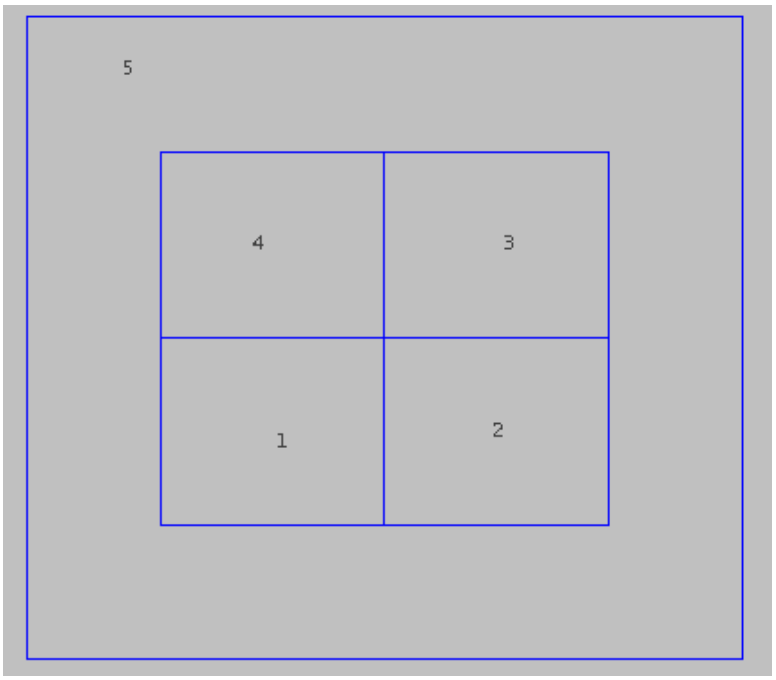

Figure 1: Geometry and media for Stepanek's benchmark.

Because of the large flux gradients, this is a very challenging benchmark for spatial discretization schemes. Tables 1 through 6 give our results for the average fluxes in media from 1 to 5 and for the total leakage, which is the quantity more difficult to get. As for the LS and the NLS, a subdivision of each surface into 4 sub-surfaces has been carried out in order to have a better approximation for the surface sources and, therefore, a well converged result. The results shown below do not claim to be reference results. All calculations have been done with the same angular quadrature formula (a product formula with 12 uniform horizontal angles between 0 and π, and 2 Gauss-Legendre vertical angles) and the same transverse spatial integration parameter δ=0.01 cm. To full understand the meaning of these parameters and evaluate their incidence on convergence we refer to [6]. What is important here is that none of these parameters can affect the convergence of the integration over a characteristic. This convergence is due only to the spatial representation of the source. Here below we will test this convergence, without asking for a fully converged result with respect to the other integration parameters. Calculations have been done on a DEC/ALPHA/4100 (EV56) 600 Mhz workstation.

The results in the tables confirm the faster convergence of the LS scheme over the standard SC scheme and the good performances of the ASA LS acceleration. The tables show that the n×n LS calculation is as precise as the 2n×2n SC one, which proves that for the same precision the LS scheme is faster. The best method is the NLS one. Actually, the NLS is the only method that gives converged values up to three significant figures for all quantities with a 128×128 mesh refinement. Its rate of convergence is much more satisfying than that of the other two methods and its n×n results are roughly as goods as the 4n×4n SC results. As for the calculation time and number of iterations, depicted in table 7, they show the good performance of the ASA LS acceleration. We have tried to apply this acceleration method also to the NLS scheme: this acceleration is unstable for the 32*32 mesh, while it converges for finer meshes, even if its behavior does not seem optimal. A stable acceleration method for the NLS scheme seems to be imperative for its extensive use, and it will be the subject of research in the next future.

Table 1: Results for the flux in medium 1 for the Stepanek benchmark. Comparison between the flat-flux (SC), the LS and the NLS schemes. Errors in % as compared to a reference value (11.94) obtained from a NLS 128×128 calculation.

Mesh (n´ n)	***16´16***	***32´32***	***64´64***	***128´128***	***256x256***
SC	-8.7	-4.3	-1.5	-0.49	-0.15
LS	6.7	1.9	0.4	0,16	
NLS	0.53	0.16	0.03	0.	

Table 2: Results for the flux in medium 2 for the Stepanek benchmark. Comparison between the flat-flux (SC), the LS and the NLS schemes. Errors in % as compared to a reference value (0.5429) obtained from a NLS 128×128 calculation.

Mesh (n´ n)	***16´16***	***32´32***	***64´64***	***128´128***	***256x256***
SC	35.2	17.8	6.6	2.02	0.38
LS	-4.3	-3.8	-1.8	-0,7	
NLS	-6.5	-1.6	-0.25	0.	

Table 3: Results for the flux in medium 3 for the Stepanek benchmark. Comparison between the flat-flux (SC), the LS and the NLS schemes. Errors in % as compared to a reference value (19.18) obtained from a NLS 128×128 calculation.

Mesh (n´ n)	***16´16***	***32´32***	***64´64***	***128´128***	***256x256***
SC	-14.7	-7.7	-2.7	-0.83	-0.21
LS	-13.5	-4.7	-1.2	-0,4	
NLS	1.1	0.26	-0.05	0.	

Table 4: Results for the flux in medium 4 for the Stepanek benchmark. Comparison between the flat-flux (SC), the LS and the NLS schemes. Errors in % as compared to a reference value (0.8369) obtained from a NLS 128×128 calculation.

Mesh (n´ n)	***16´16***	***32´32***	***64´64***	***128´128***	***256x256***
SC	41.9	21.	7.8	2.3	0.48
LS	29.3	9.1	1.7	0,13	
NLS	-3.1	-0.92	-0.2	0.	

Table 5: Results for the flux in medium 5 for the Stepanek benchmark. Comparison between the flat-flux (SC), the LS and the NLS schemes. Errors in % as compared to a reference value (1.5269) obtained from a NLS 128×128 calculation.

Mesh (n´ n)	***16´16***	***32´32***	***64´64***	***128´128***	***256x256***
SC	16.9	13.4.	6.6	2.3	0.6
LS	27.9	16.6	5.6	1.2	
NLS	-0.03	-0.013	0.013	0.	

Table 6: Results for the total leakage for the Stepanek benchmark. Comparison between the flat-flux (SC), the LS and the NLS schemes. Errors in % as compared to a reference value (8.751) obtained from a NLS 128×128 calculation: [a] computation time (sec), [b] number of internal iterations with the ASA acceleration, [c]. number of internal iterations without ASA.

Mesh (n´ n)	***16´16***	***32´32***	***64´64***	***128´128***	***256x256***
SC	503.	209.	63.9	17.5	4.3
LS	111.	55.5	18.7	3.7	
NLS	6.2	1.5	0.42	0.	
SC	4.6 [a] **6** [b]	18.59 [a] **8**	70.7 [a] **10**	605 [a] **18**	1740 [a]
LS	12.74 [a] **7**	47.16 [a] **9**	181.2 [a] **12**	2510 [a] **19**	
NLS	1678 [c] **773**	3746 [c] **831**	390 [a] **27**	1678 [a] **43**	

6. CONCLUSIONS

Two new spatial discretization methods (LS and NLS) have been developed for the MOC, and the synthetic ASA acceleration has been modified to work with one of these methods (LS). Our numerical tests prove that the new LS and NLS methods are efficient and fast for reactor applications. For slab geometry the LS method is alike to the familiar linear continuous (LC) method [4] used in regular meshes. Therefore, this new method can be viewed as a generalization to non-structured meshes of the LC scheme. On the other hand, the NLS is a positive, nonlinear method with higher-order convergence properties. Due to its non-linearity it is quite difficult to accelerate. In this paper we show that even if not stable the LS ASA method can be effective for sufficiently fine mesh refinements. We hope in the future to be able to "stabilize" the technique.

We think that the new scheme will be of practical interest in reactor calculations, and we aim to extend its applications to realistic multigroup calculations.

7. REFERENCES

[1] R. Sanchez and A. Chetaine, "A Synthetic acceleration for a two dimensional characteristic method in unstructured meshes" *Nuc. Sci. Eng*., **136**, 122-139, 2000.
[2] S. Santandrea and R. Sanchez, "Acceleration Techniaues for the characteristiques metos in unstructured meshes" *Ann. of Nuc. Ene.*, **29**, 323-352, 2002.
[2] Walters and Wareing, *Transp.* "An Accurate Strictly Positive Nonlinear Characteristic Scheme for the Discrete Ordinate equation" *Theory and Stat. Physics*, **25**, 2, 197, 1996.
[3] J. Stepanek et al.,.Calculation of four thermal benchmarks in xy geometry, EIR-Bericht Nr 464, Federal Institute of Technology (ETH), 1982.
[4] E.E. Lewis and W.F. Miller, Jr., Computational Methods of Neutron Transport, *American Nuclear Society Inc*., 1993.
[5] Y. Saad, *"Iterative Methods for Sparse Linear Systems",* PWS Publishing Company, Boston, Massachusetts (1996).
[6] R. Sanchez, L. Mao and S. Santandrea, "Treatment of Boundary conditions in trajectory Based Deterministic Transport Methods", *Nuc. Sci. Eng*.,**140**,1,2002